



# Synthesis and characterization of thermally evaporated copper bismuth sulphide thin films

Arshad Hussain<sup>a,\*</sup>, R. Ahmed<sup>a,\*</sup>, Nisar Ali<sup>a</sup>, Naser M AbdEl-Salam<sup>b</sup>, Karim bin Deraman<sup>a</sup>, Yong Qing Fu<sup>c,\*</sup>

<sup>a</sup> Department of Physics, Faculty of Science, University Teknologi Malaysia, Skudai 81310, Johor, Malaysia

<sup>b</sup> Ar-Riyadh Community College, King Saud University, Riyadh 11437, Saudi Arabia

<sup>c</sup> Faculty of Engineering and Environment, Northumbria University, Newcastle upon Tyne NE1 8ST, UK

## ARTICLE INFO

### Article history:

Received 31 August 2016

Revised 1 December 2016

Accepted in revised form 3 December 2016

Available online 7 December 2016

### Keywords:

Cu<sub>3</sub>BiS<sub>3</sub>

Thermal deposition

Photoluminescence

Optical band gap

Transmittance

## ABSTRACT

Non-toxic copper containing chalcogenides are considered as promising alternate materials for the absorber layer in thin film solar cells and visible-light harvesting devices. In this paper, we reported synthesis of Cu<sub>3</sub>BiS<sub>3</sub> thin films using a two-step thermal evaporation method for the first time. A Cu<sub>2</sub>S layer of 0.4 μm thickness was firstly evaporated onto glass substrate at room temperature, followed by evaporation of a Bi<sub>2</sub>S<sub>3</sub> layer of 0.8 μm thickness. The Cu<sub>3</sub>BiS<sub>3</sub> thin films were formed by thermally annealing and diffusing the two evaporated layers in a vacuum furnace. This method resulted in the improved crystallinity and phase purity of the grown Cu<sub>3</sub>BiS<sub>3</sub> films. Effects of annealing temperature on different properties of the fabricated samples were investigated. The obtained low band-gap (1.45 eV) and good optical properties such as low transmittance (10–30%) and reflectance (~10%) of the Cu<sub>3</sub>BiS<sub>3</sub> films demonstrated it as a suitable material for the absorber layer of solar cells.

© 2017 The Authors. Published by Elsevier B.V. This is an open access article under the CC BY license (<http://creativecommons.org/licenses/by/4.0/>).

## 1. Introduction

The photovoltaic modules based on thin film solar cells such as CdTe and Cu(In,Ga)Se<sub>2</sub> have shown high efficiencies exceeding 22% [1,2], however, their toxicity has been a critical issue [3]. Moreover, large-scale manufacture of thin film solar panels requires cheap, earth-abundant and environment-friendly materials to be used as viable sources of green energy for the community. Among the newly developed, low cost and nontoxic materials, copper zinc tin sulphide (CZTS) is an emerging material with an efficiency of ~12%, however, there are still many complications associated with the CZTS. For example, its narrow single-phase region in the phase diagram and its multiple secondary phases within the material limit the further improvement in its cell efficiency [4,5].

In recent years investigations have begun to focus on another earth-abundant and less-toxic ternary semiconductor compound called copper bismuth sulphide (Cu<sub>3</sub>BiS<sub>3</sub>). It belongs to I-V-VI group and is naturally found in the Wittichenite mineral with an orthorhombic structure (a = 0.7725 nm, b = 1.0395 nm, and c = 0.6716 nm). It was reported to be one of the suitable materials for the solar cell absorber layer [6,7]. Fabrication of the Cu<sub>3</sub>BiS<sub>3</sub> (CBS) thin films was reported by different research groups for solar cell applications using various techniques such as sputtering, evaporation, combined chemical and thermal

approach, and solid state reactions [7–10]. It was reported that the CBS films have a stable structure at room temperature and an energy band gap of 1.4 eV, which is pretty close to the best region in the visible solar energy spectrum thus suitable for the photovoltaic applications [11]. The most common feature of the Cu<sub>3</sub>BiS<sub>3</sub> is the presence of localized states due to inherent defects in the mobility gap, along with its polycrystalline nature [10]. P-type conductivity of the CBS samples was reported by Mesa et al. [12]. The same group also reported a Hall mobility of 4 cm<sup>2</sup>/V s, a carrier concentration of  $2 \times 10^{16}$  cm<sup>-3</sup> and a thermoelectric power output of ~0.73 mV/K for the thermally co-evaporated Cu<sub>3</sub>BiS<sub>3</sub> thin films [13]. Cu<sub>3</sub>BiS<sub>3</sub> thin films was also prepared by post-annealing the magnetron sputtered Cu and Bi layer with a thermally evaporated S layer, and the film was reported to have p-type conductivity, good lateral homogeneity, and Wittichenite orthorhombic structure with a direct band gap [14].

In this work, we report, for the first time, the fabrication of Cu<sub>3</sub>BiS<sub>3</sub> thin films using a novel two-step thermal evaporation technique (i.e., successive deposition of Cu<sub>2</sub>S and Bi<sub>2</sub>S<sub>3</sub> layers) followed by post-annealing in vacuum. The structural, morphological, and optical properties of the annealed films are characterized.

## 2. Experimental

Soda lime glass substrates were cleaned with acetone and methanol, rinsed with deionized water, and then dried with nitrogen gas. A two-step thermal evaporation technique was employed for successively depositing Cu<sub>2</sub>S and Bi<sub>2</sub>S<sub>3</sub> pellets of 99.99% purity onto glass substrates.

\* Corresponding authors.

E-mail addresses: [harshad.utm@gmail.com](mailto:harshad.utm@gmail.com) (A. Hussain), [rashidahmed@utm.my](mailto:rashidahmed@utm.my) (R. Ahmed), [Richard.fu@northumbria.ac.uk](mailto:Richard.fu@northumbria.ac.uk) (Y.Q. Fu).

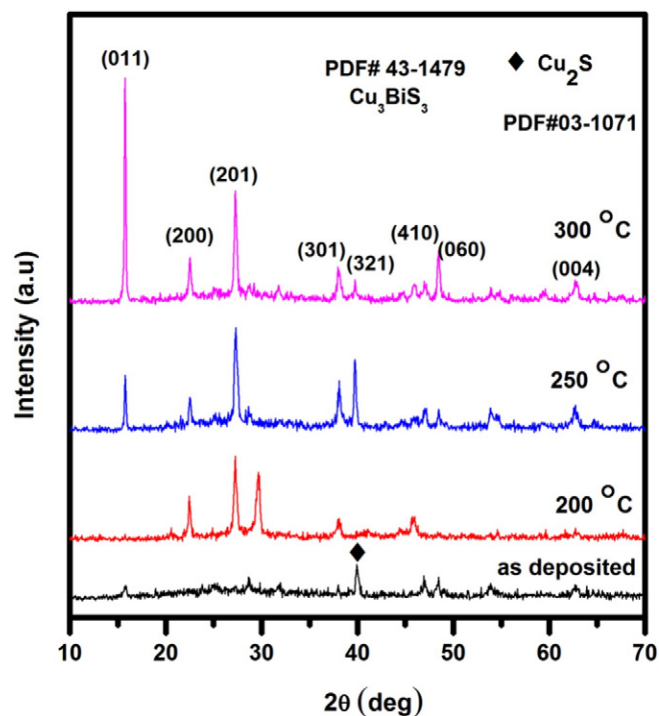


Fig. 1. XRD analysis of the as-deposited and annealed  $\text{Cu}_3\text{BiS}_3$  films.

Both pallets were evaporated in a vacuum chamber at a pressure of  $5 \times 10^{-5}$  mbar from a tungsten crucible connected to a power supply. A  $\text{Cu}_2\text{S}$  layer of 400 nm thickness was firstly deposited by supplying a current of 95 A and then a  $\text{Bi}_2\text{S}_3$  layer of 800 nm thickness was deposited

on top of the  $\text{Cu}_2\text{S}$  layer, thus obtaining a film of 1.18  $\mu\text{m}$  thickness. The  $\text{Cu}_3\text{BiS}_3$  thin films were then obtained by thermally annealing the  $\text{Cu}_2\text{S}$  and  $\text{Bi}_2\text{S}_3$  double layers at different temperatures of 200  $^\circ\text{C}$ , 250  $^\circ\text{C}$  and 300  $^\circ\text{C}$  for 60 min in a vacuum furnace to study the effect of thermal annealing on the structural and optical properties of the fabricated films. Structural characterization of the films was carried out using the X-ray D-8 Discover diffractometer with Cu radiation ( $k\text{-}\alpha$  lines  $\lambda = 1.54 \text{ \AA}$ ). Surface morphology of the as-deposited and annealed samples was investigated using a field emission scanning electron microscope (FESEM, SU8020 X-Max<sup>N</sup> Oxford). Energy dispersive X-ray spectroscopy (EDX) with a probe current of 5.0 nA was used for elemental analysis. The UV–Vis spectroscopy was carried out for the optical characterization of the thin films using Shimadzu, UV 3101pc UV-VIS-NIR spectrometer. The four-probe technique using a programmable Keithly 2400 source meter was used for the electrical characterization of the thin films. The electrical contacts were made on the thin film surface using adhesive silver conductive paint and the measurement were performed with gradually increasing applied voltage up to 5 V. The photoluminescence (PL) spectra were obtained using a Perkin Elmer, LS5 photoluminescence spectrometer.

### 3. Results and discussion

Fig. 1 shows the XRD patterns for the as-deposited and annealed samples. The as-deposited film has a crystalline phase of  $\text{Cu}_2\text{S}$  based on the standard XRD card PDF#03-1071. Similarly, all the peaks observed in the annealed samples are well matched with the standard PDF#43-1479 (Using X'Pert HighScore software), for the Wittichenite  $\text{Cu}_3\text{BiS}_3$  phase, and no secondary phases were observed. The crystallite size predicted using the Scherrer formula for the (011) peak at  $2\theta = 15.75^\circ$  was  $\sim 44 \text{ nm}$  for the film annealed at 300  $^\circ\text{C}$ .

Due to the low melting point of bismuth (271  $^\circ\text{C}$ ), it is expected that the bismuth will be diffused throughout the thickness of the films. From

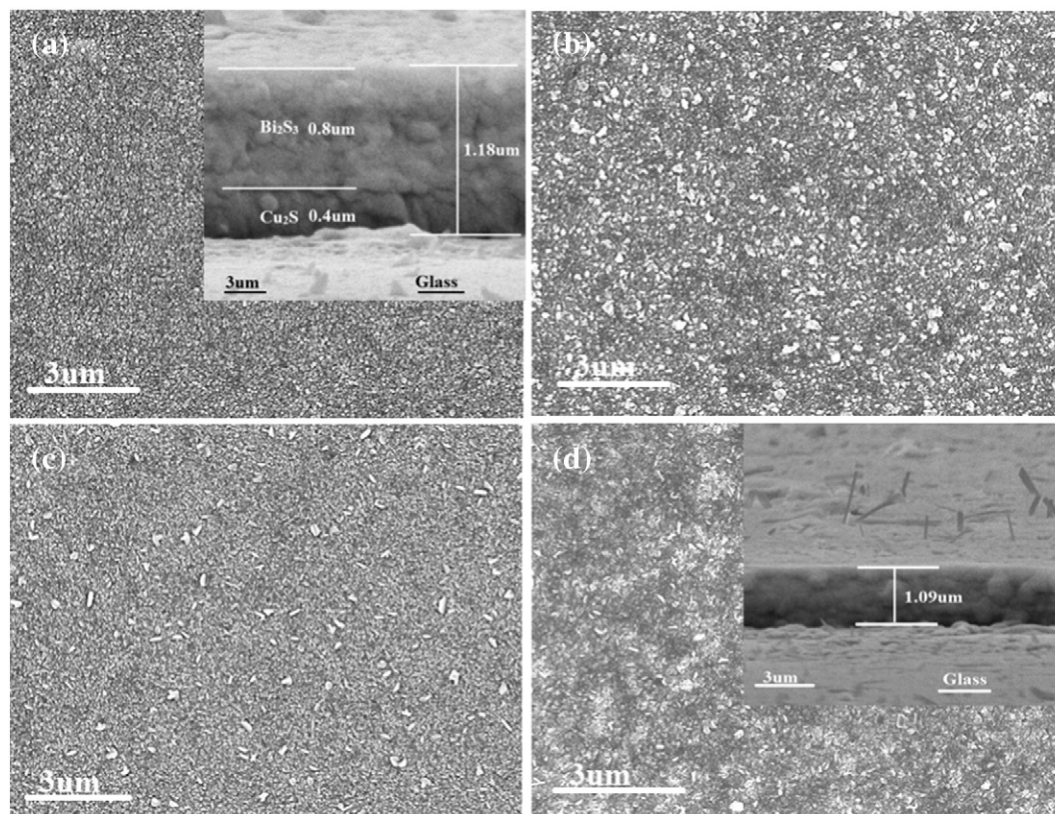


Fig. 2. Scanning electron micrographs of (a) as-deposited sample (b) 200  $^\circ\text{C}$  annealed sample (c) 250  $^\circ\text{C}$  annealed sample (d) 300  $^\circ\text{C}$  annealed sample and inset of (d) show the cross-sectional view of the sample.

**Table 1**  
Elemental composition extracted from EDX spectra.

Element	At (%)	wt (%)	$\sigma$
Cu	45.23	40.27	4.90
Bi	14.17	41.49	3.97
S	40.61	18.25	4.42

the XRD results, it is also found that the crystallinity of the  $\text{Cu}_3\text{BiS}_3$  thin films increases with an increase in the annealing temperature due to grain growth. Similar behavior has also reported by Veronica et al. [7], for the CBS films fabricated using a solid-state reaction method however in our work, the CBS films show much better crystalline quality, i.e., the larger grain size. The average crystallite sizes calculated using the Debye-Scherrer formula [15,16] was found to be consistent with those from the FESEM micrographs as shown in Fig. 2.

From the FESEM image shown in Fig. 2(a), the surface of the as-deposited film consists of the smooth distribution of microstructural features. However, after annealing and with the increase of the annealing temperature, the agglomeration of structures and increase of the crystallite size can be observed from Fig. 2(b). Further annealing up to 250 °C results in rough surface features with some un-agglomerated particles as shown in Fig. 2(c). When the annealing temperature is increased further to 300 °C, all the voids between the grains are filled up and correspondingly a uniformly distributed and compact surface can be observed as shown in Fig. 2(d). The shape of the surface particles turns into spherical which might be able to lead to a reduction in recombination loss during PV process [16,17]. Inset of Fig. 2 (a) and (d) shows the enlarged cross-sectional micrographs of the as-deposited thin film and the one annealed at 300 °C, respectively. As can be seen from the inset of Fig. 2 (a), two different layers of  $\text{Cu}_2\text{S}$  and  $\text{Bi}_2\text{S}_3$  with thicknesses of 0.4  $\mu\text{m}$  and 0.8  $\mu\text{m}$  can be observed, resulting in the thickness of the thin film of about 1.18  $\mu\text{m}$  with a uniform distribution. After annealing the obtained  $\text{Cu}_3\text{BiS}_3$  thin films have been changed into a single homogeneous layer which can be observed from the inset of Fig. 2(d). There are no clear voids and spikes showing a good film adhesion with the substrate. The calculated thickness of the thin film annealed at 300 °C was  $\sim 1.09 \mu\text{m}$ , as shown in the inset Fig. 2(d).

EDX analysis shows the Cu, Bi and S elements in the thin film with an atomic ratio of around 3: 1: 3. The composition data of the constituent elements of the sample in atomic and weight percentages with possible errors in the measurement are listed in Table 1.

The optical reflectance and transmittance properties of the as-deposited and annealed films are shown in Figs. 3 and 4 respectively in

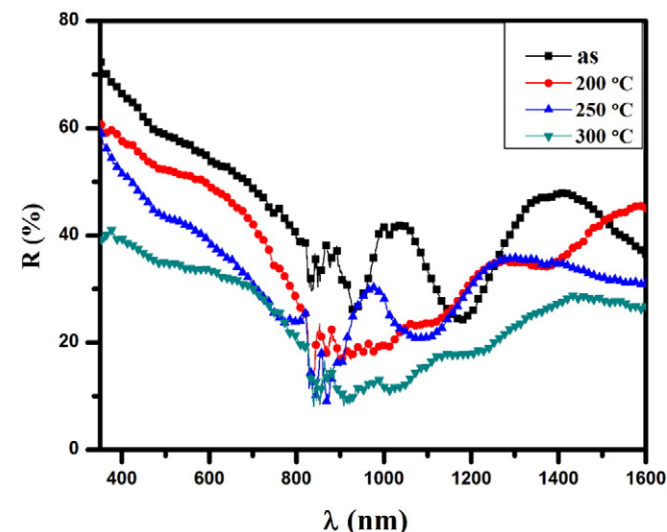


Fig. 3. Reflectance spectroscopy of as-deposited and annealed  $\text{Cu}_3\text{BiS}_3$  thin films.

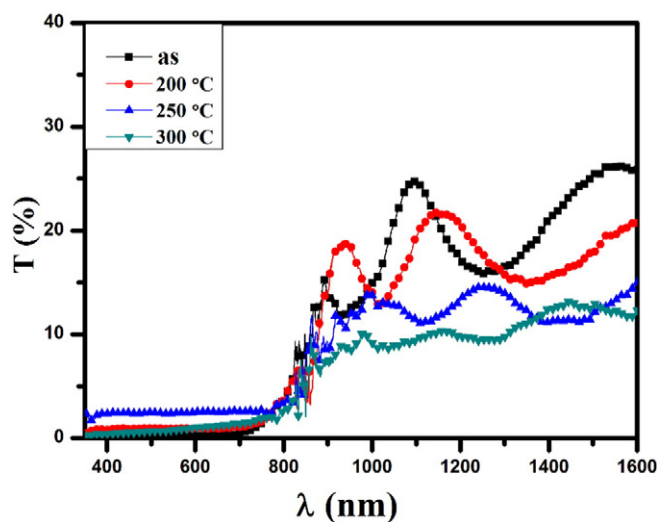


Fig. 4. Transmittance spectra of the as-deposited and annealed  $\text{Cu}_3\text{BiS}_3$  samples.

the wavelength range of 350–1600 nm. The reflectance of the samples (shown in Fig. 3) was observed to decrease (75% to 40%) in the visible wavelength region which is attributed to the enhancement of absorption with regularly arranged crystal orientations due to the increased annealing temperature. The reflectance is uniform in the wavelength range of 350–820 nm but is wavy shaped in the range of 820–1600 nm, revealing the homogeneity of the films. The reflection of the 300 °C annealed film shows the lowest value in the visible and NIR part of the spectrum 350–850 nm. Such a low reflectance is highly preferred for solar cell materials. The transmittance spectra of the as-deposited and annealed samples are shown in Fig. 4. It shows decreased value (30–10%) in the wavelength range of 820–1600 nm. However, the transmittance in the visible region of the spectrum is lowest for all the as-deposited and annealed samples, indicating the good absorption capability of the samples.

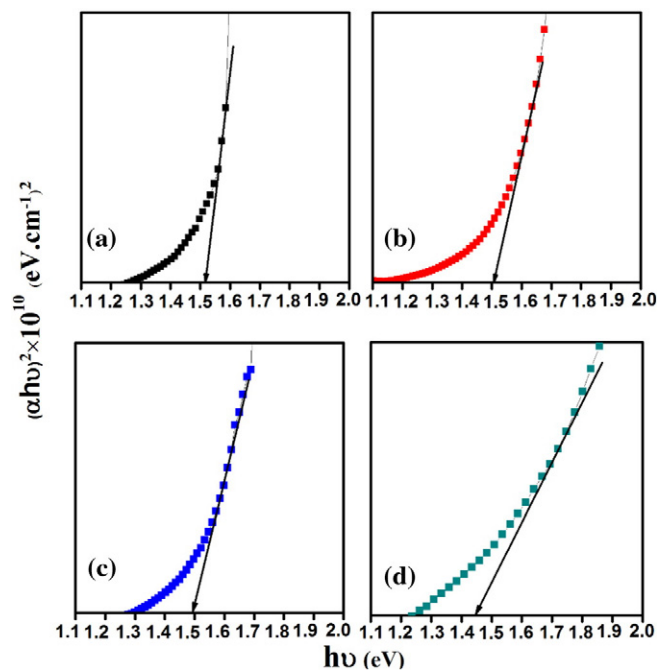


Fig. 5. Band gap calculation for as grown and annealed  $\text{Cu}_3\text{BiS}_3$  thin films.



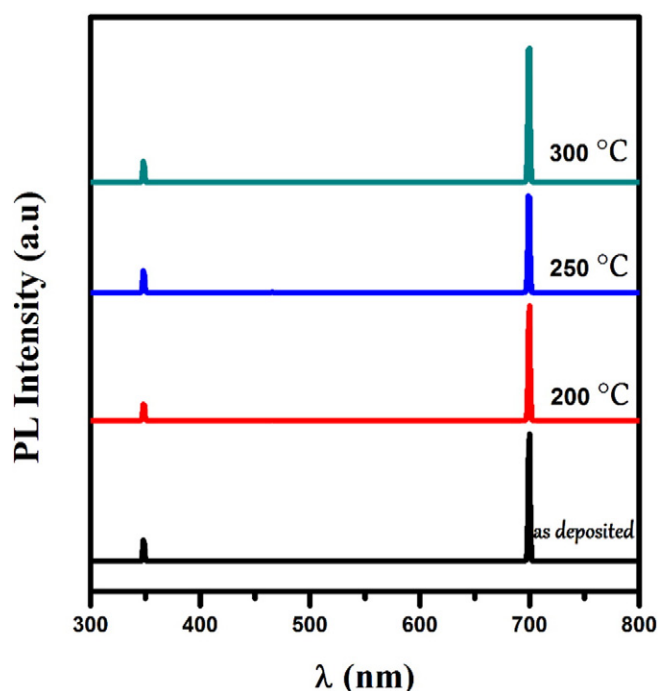


Fig. 6. Photoluminescence spectroscopy of the fabricated  $\text{Cu}_3\text{BiS}_3$  thin films.

The optical band gap energies (Fig. 5) were calculated by the standard Tauc's relation [12,18,19]:

$$(\alpha h\nu)^n = A (h\nu - E_g) \quad (1)$$

where  $E_g$  is the optical band gap energy,  $\alpha$  is the absorption coefficient at a frequency of  $\nu$ ,  $A$  is constant and  $n = 2$  and  $1/2$  for allowed direct and indirect transitions correspondingly. The optical absorption co-efficient was calculated using the following relation:

$$\alpha = \frac{1}{d} \ln \left[ \frac{(1-R)^2}{T} \right] \quad (2)$$

where  $d$ ,  $R$ , and  $T$  are for the thickness, reflectance spectra and transmittance spectra of the fabricated  $\text{Cu}_3\text{BiS}_3$  thin films, respectively. The

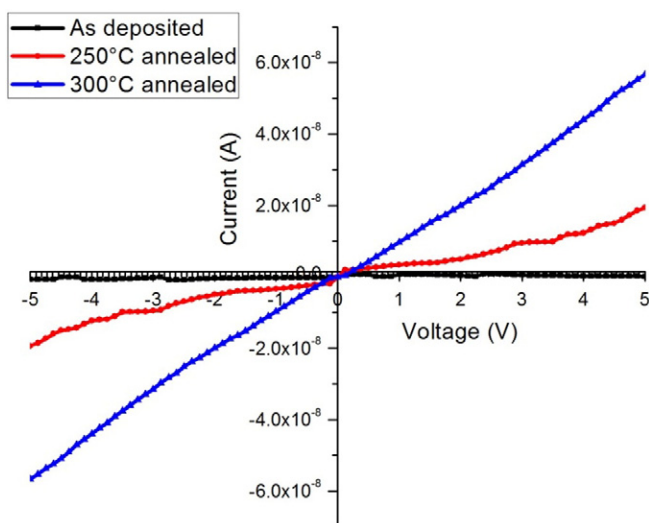


Fig. 7. The transverse current–voltage characteristics of as-deposited and annealed  $\text{Cu}_3\text{BiS}_3$  thin films.

optical band gap of the sample annealed at 200 °C calculated from the Tauc's plot is 1.51 eV, while it decreases to 1.45 eV for the sample annealed at 300 °C. All the data shows that the films are suitable for the absorber layer in thin film solar cells. The band gap values are similar with those reported in the literature [10,13,19,20]. At a high annealing temperature, the grain growth and reduction in the impurities are responsible for the decrease in the band gap values [21].

The PL spectroscopy analysis results of the grown samples are shown in Fig. 6. There are slight shifts toward the lower wavelength region (blue shift) observed in the PL spectra with the increase of annealing temperature. The variation of the PL spectra with increasing annealing temperature is an indication of carrier de-trapping from localized extended states [22]. The peak shift is also an indication of the existence of shallow energy level.

Fig. 7 shows the I–V curves for the as-deposited and post annealed  $\text{Cu}_3\text{BiS}_3$  thin films. The linear relationship between the current and voltage is obtained and the current is observed to increase with increasing annealing temperature due to the reduction of grain boundaries and improvement of crystallinity. The electrical resistivity was observed to decrease with annealing temperature, hence the increase in electrical conductivity at higher temperature may be attributed to the reduction of potential barriers generated by the grain boundaries thus resulting in an increase in the electrical conductivity of the films [21,23].

#### 4. Conclusions

The  $\text{Cu}_3\text{BiS}_3$  films were synthesized using thermal evaporation technique and annealed at moderate temperatures from 200 to 300 °C. The crystallinity and crystallite size in the thin films were observed to be increased with the increase in annealing temperature based on the XRD analysis. The measured energy band gap value, 1.45 eV at 300 °C for the  $\text{Cu}_3\text{BiS}_3$  thin films exhibited it as a potential ideal material for photovoltaic applications. The lower reflectance ( $\sim 10\%$ ) from the surface of the thin films indicates the homogeneity and smoothness of the films. The FESEM images also confirmed the grain growth and homogeneity of the films. The I–V curves show the photovoltaic nature of  $\text{Cu}_3\text{BiS}_3$  thin films, therefore, the prepared CBS thin films can be used as an absorber layer in photovoltaics.

#### Acknowledgements

The authors would like to thank University Teknologi Malaysia/Ministry of Education Malaysia for the financial support of this research work through project nos. QJ130000.2526.12H46, RJ130000.7826.4F508, and International Doctoral Fellowship/UTM IDF and the author (Naser M Abdel-Salam) is thankful to the Deanship of Scientific Research at King Saud University for funding the work through the research group project No. RGP-210. Richard Fu acknowledges the support from UK EPSRC funding EP/P018998/1.

#### References

- [1] M.A. Green, et al., Solar cell efficiency tables (version 47), Prog. Photovolt. Res. Appl. 24 (1) (2016) 3–11.
- [2] N. Ali, et al., Advances in nanostructured thin film materials for solar cell applications, Renew. Sust. Energ. Rev. 59 (2016) 726–737.
- [3] M. Yakushev, et al., Investigation of the structural, optical and electrical properties of  $\text{Cu}_3\text{BiS}_3$  semiconducting thin films, Energy Procedia 60 (2014) 166–172.
- [4] W. Wang, et al., Device characteristics of CZTSSe thin-film solar cells with 12.6% efficiency, Adv. Energy Mater. 4 (7) (2014).
- [5] S. Siebentritt, S. Schorr, Kesterites—a challenging material for solar cells, Prog. Photovolt. Res. Appl. 20 (5) (2012) 512–519.
- [6] V. Kocman, E. Nuffield, The crystal structure of wittichenite,  $\text{Cu}_3\text{BiS}_3$ , Acta Crystallogr. B Struct. Crystallogr. Cryst. Chem. 29 (11) (1973) 2528–2535.
- [7] M. Nair, P. Nair, Semiconducting  $\text{Cu}_3\text{BiS}_3$  thin films formed by the solid-state reaction of CuS and bismuth thin films, Semicond. Sci. Technol. 18 (2) (2003) 190.
- [8] N.J. Gerein, J.A. Haber, One-step synthesis and optical and electrical properties of thin film  $\text{Cu}_3\text{BiS}_3$  for use as a solar absorber in photovoltaic devices, Chem. Mater. 18 (26) (2006) 6297–6302.

- [9] H. Hu, O. Gomez-Daza, P. Nair, Screen-printed Cu<sub>3</sub>BiS<sub>3</sub>-Polyacrylic acid composite coatings, *J. Mater. Res.* 13 (09) (1998) 2453–2456.
- [10] F. Mesa, A. Dussan, G. Gordillo, Evidence of trapping levels and photoelectric properties of Cu<sub>3</sub>BiS<sub>3</sub> thin films, *Phys. B Condens. Matter* 404 (23) (2009) 5227–5230.
- [11] F. Mesa, et al., Transient surface photovoltage of p-type Cu<sub>3</sub>BiS<sub>3</sub>, *Appl. Phys. Lett.* 96 (2010) 082–113.
- [12] F. Mesa, G. Gordillo, Effect of preparation conditions on the properties of Cu<sub>3</sub>BiS<sub>3</sub> thin films grown by a two-step process, *Journal of Physics: Conference Series*, IOP Publishing, 2009.
- [13] F. Mesa, et al., Transient surface photovoltage of p-type Cu<sub>3</sub>BiS<sub>3</sub>, *Appl. Phys. Lett.* 96 (8) (2010) 2113.
- [14] M. Yakushev, et al., Electronic and structural characterisation of Cu<sub>3</sub>BiS<sub>3</sub> thin films for the absorber layer of sustainable photovoltaics, *Thin Solid Films* 562 (2014) 195–199.
- [15] N. Ali, et al., Effect of air annealing on the band gap and optical properties of SnSb<sub>2</sub>S<sub>4</sub> thin films for solar cell application, *Mater. Lett.* 100 (0) (2013) 148–151.
- [16] S. Subramanian, et al., Electron beam induced modifications of bismuth sulphide (Bi<sub>2</sub>S<sub>3</sub>) thin films: structural and optical properties, *Radiat. Phys. Chem.* 79 (11) (2010) 1127–1131.
- [17] J. Li, et al., Electrodeposition and characterization of copper bismuth selenide semiconductor thin films, *Electrochim. Acta* 87 (2013) 153–157.
- [18] M. Kumar, C. Persson, Cu<sub>3</sub>BiS<sub>3</sub> as a potential photovoltaic absorber with high optical efficiency, *Appl. Phys. Lett.* 102 (6) (2013) 062109.
- [19] F. Mesa, A. Dussan, G. Gordillo, Study of the growth process and optoelectrical properties of nanocrystalline Cu<sub>3</sub>BiS<sub>3</sub> thin films, *Phys. Status Solidi C* 7 (3–4) (2010) 917–920.
- [20] F. Mesa, et al., Study of Cu<sub>3</sub>BiS<sub>3</sub> Thin films prepared by co-evaporation Proceedings of the 24th European Photovoltaic Solar Energy Conference, 2009.
- [21] N. Ali, et al., Advances in nanostructured thin film materials for solar cell applications, *Renew. Sust. Energ. Rev.* 59 (2016) 726–737.
- [22] J.K. Saluja, et al., Mechano and photoluminescence spectra of cadmium sulphide and cadmium selenide doped phosphors, *Optik* 127 (19) (2016) 7958–7966.
- [23] G. Rusu, M. Rusu, On the electrical conductivity of CdTe thin films evaporated onto unheated substrates, *Solid State Commun.* 116 (7) (2000) 363–368.